Supporting Information

Increasing Cancer Therapy Efficiency Through Targeting And Localized Light Activation

Yuqi Yang,[†,‡] Shizhen Chen, [†,‡] Lianhua Liu, [‡] Sha Li,[‡] Qingbin Zeng, [‡] Xiuchao Zhao,[‡] Haidong Li, [‡] Zhiying Zhang, [‡] Louis-S. Bouchard,[§] Maili Liu[‡] and Xin Zhou*[,‡]

[‡]Key Laboratory of Magnetic Resonance in Biological Systems, State Key Laboratory of Magnetic Resonance and Atomic and Molecular Physics, National Center for Magnetic Resonance in Wuhan, Wuhan Institute of Physics and Mathematics, Chinese Academy of Sciences, Wuhan, 430071, P. R. China.

[§]Departments of Chemistry and Biochemistry and of Bioengineering, California NanoSystems Institute, The Molecular Biology Institute, Jonsson Comprehensive Cancer Center, University of California, Los Angeles, CA 90095 USA.

* E-mail: xinzhou@wipm.ac.cn

Experimental Section

Materials and Instrumentation. Multiwall carbon nanotubes (MCNT) were purchased from Nanjing XFNANO Materials Tech Co., Ltd (Nanjing, China). N-(3-Dimethylaminopropyl)-N-ethyl-carbodimide hydrochloride (EDC•HCl, 99%), N-Hydroxysuccinimide (NHS, 97%), benzyl 4-2'-methoxycarbonyl-ethyl-3,5-dimethylpyrole-2-carboxylate, dimethyl-formamide, 3,4-diethyl pyrrole, gadolinium(III) chloride hexahydrate ($GdCl_3$•$6H_2O$, 99%), Lutetium(III) nitrate hydrate ($Lu(NO_3)_3 \cdot xH_2O$) and poly(ethylene glycol) bis(amine) (PEG-diamine, Mr 2000) were purchased from Sigma-Aldrich (St. Louis, USA). Triethyl orthotomate and 3, 4-Diaminophenol were purchased from J&K Scientific. c(RGDyK) (cyclo(Arg-Gly-Asp-d-Phe-Lys)) was purchased from GL Biochem (Shanghai, China). Dialysis bag (Mr 3500Da) was purchased from Biosharp (Hefei, China). Human lung adenocarcinoma cell line A549 and breast cancer cell line MCF7 were obtained from the Cell Bank of Chinese Academy of Sciences (Shanghai, China). Nucleic acid stains Hoechst 33342 and Sytox Green were purchased from Life Technologies. Cytomembranestains DiSC3 (Ex/Em 660/675 nm) and DiO (Ex/Em 484/501 nm) were purchased from AAT Bioquest Inc. (Sunnyvale, CA, USA).

A microwave system Monowave 300 was used for synthesizing graphene quantum dots (GQD) (Anton Paar, Austria). Exclusive vitreous vessels with a volume of 10 mL were equipped for the system to provide security during reaction demanding high temperature and pressure. The synthesized GQD was characterized by transmission electron microscopy (TEM, JEM-2100), high resolution transmission electron microscopy (HTEM, Tecnai G2 F20 U-TWIN) and Atomic Force Microscope (Vecco digital instruments, di Innova). The chemical compositions of MCNT and GQD were determined by an ESCALAB 220i-XL X-ray photoelectron spectrometer (XPS)

(VG Scientific Ltd.). UV-vis absorption spectra were recorded on an Evolution 220 spectrophotometer (Thermo fisher scientific). Fluorescence spectra were recorded at room temperature on an Edinburgh FS5 fluorescence spectrophotometer. The concentration of cells was confirmed by an autocellometerK2 from Nexcelom (Lawrence, MA, USA). All fluorescent imaging experiments on cells were performed on a laser scanning confocal microscope Nikon A1 (Nikon, Tokyo, Japan). Fluorescence imaging of mice was performed on a Bruker In-Vivo Xtreme-Optical and X-ray Small Animal Imaging System.

MRI was performed using a 7 T small animal horizontal bore system (Bruker BioSpec, Billerica, MA). A red diode laser MDL-III with wavelength of 765 nm (maximum power, 1 W) was purchased from Changchun New Industries Optoelectronics Co., Ltd (Changchun, China). Laser power was detected by a laser power meter FieldMax (Coherent Inc., Santa Clara, CA, USA). An infrared thermal imager HS 160 from DALI Technology (Hangzhou, China) was used to monitor the change of temperature during irradiation.

Synthesis of grahene quantum dots (GQD). A two-step approach was employed to fabricate orange-emitting GQD. First, multi-wall carbon nanotubes (50 mg) were suspended in a mixture of 98% sulfuric acid (50 mL), fuming nitric acid (15 mL) and distilled water (5 mL) by sonication. After 24 h heating at 70 °C, the mixture was cooled to room temperature and diluted with 250 mL deionized water. The obtained solution was antagonized by Na_2CO_3 and then filtrated to remove the precipitated salt. Redundant salt were removed by dialysis against distilled water, and the obtained solution was evaporated to 50 mL and freeze dried. Second, the oxidized MCNT were cut into GQD by a microwave-assisted hydrothermal method. The obtained brown powder was dispersed in DMF by 30 minsonication (120 W, 100 kHz). 6 mL of

the mixed solution was transferred to the exclusive vitreous vessel with a volume of 10 mL. Orange emission GQD was prepared under 200 ºC for 20 min. After cooling to room temperature, the obtained mixture was filtered through a 0.22 μm microporous filter. A brown solution was obtained by washing the used microporousfilter with distilled water. Large fragments were eliminated by filtering the solution with a 0.02 μm anopore inorganic membrane (AnodiscTM, Watman). To further remove the DMF residues,the obtained GQD aqueous solution was further dialyzed for 48 h in high purity water.

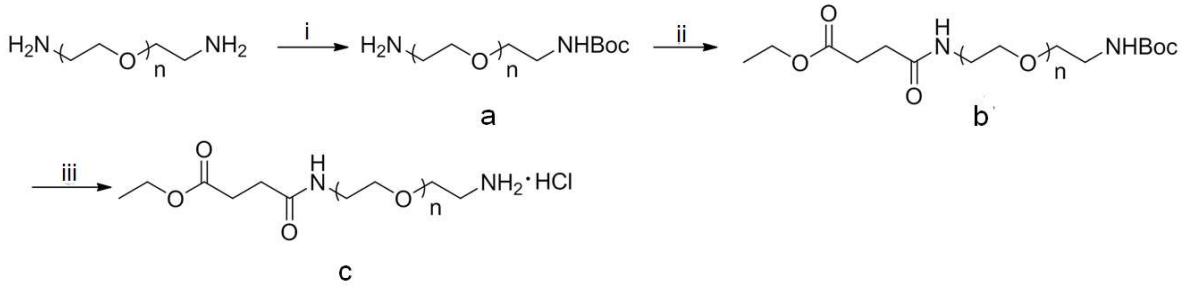

Scheme S-1. Synthesis of EtO-PEG-NH_2

Synthesis of PEG-Boc (a). Di-tert-butyl dicarbonate (0.4 mmol) was added to PEG 2000 (1.0 mmol) in THF at 0 °C. After 30 min stirring in the cooling bath, the mixture was further stirred at room temperature overnight. The precipitate was filtered, and the filtrate was washed with brine for three times. The solution was dried by Na_2SO_4 and concentrated to get the protection product **a**.

EtO-PEG-Boc (b). Mono-ethyl succinate (1 mmol) was dissolved in CH_2Cl_2 at 0 °C and stirred 10 min. Then HOBT (1.2 eq) and EDCI hydrochloride (1.2 eq) were added to the mixture. After 30 min, PEG-2000-Boc (compound a) (1 eq) and Et_3N (4.0 eq) were added and stirred

overnight at room temperature. The mixture was diluted with water and CH_2Cl_2 (10 mL), the organic layer was washed with brine, dried over Na_2SO_4 and concentrated to get the crude product **b**.

EtO-PEG-NH_2 (c). EtO-PEG-2000-Boc (compound **b**) was dissolved in 3 M HCl (g)/EtOAc and reacted for 30 min at room temperature. The resulting solution was then evaporated and the obtained residue was compound **c**.

Synthesis of GQD-RGD. To fabricate a smart vehicle that could identify non-small cell lung carcinoma A549, we linked targeted peptide RGD to GQD through a PEG bridge.

191 mg EDC and 10mg GQD were placed in a 50 mL round-bottom flask with 10 mL distilled water. The pH was adjusted to 5.0 by 0.1 mM HCl. After 10 min sonication and 2 h stirring at room temperature, pH was then adjusted to 8.0 by 0.1 mM NaOH. Then 28.75 mg NHS and 50 mg EtO-PEG-NH_2 in 10 mL DMF was added. The mixture was stirred for another 24 h at room temperature. The produced GQD-PEG-OEt solution was purified by dialysis against distilled water. To hydrolyze the ester group, 2.5 mg KOH was added to a mixture of distilled water and methanol (1:1) solution which dispersed the freeze dried GQD-PEG-OEt. After reacted overnight, excess small molecules were removed by dialysis. RGD was further modified to the GQD nanoparticles by reaction between the carboxyl groups of GQD-PEG-COOH and the amino groups of RGD. The GQD-RGD was characterized by UV−vis spectra. GQD showed a small absorption peak around 460 nm, an increased peak at 276 nm revealed successful linkage of RGD to GQD (Figure S-1).

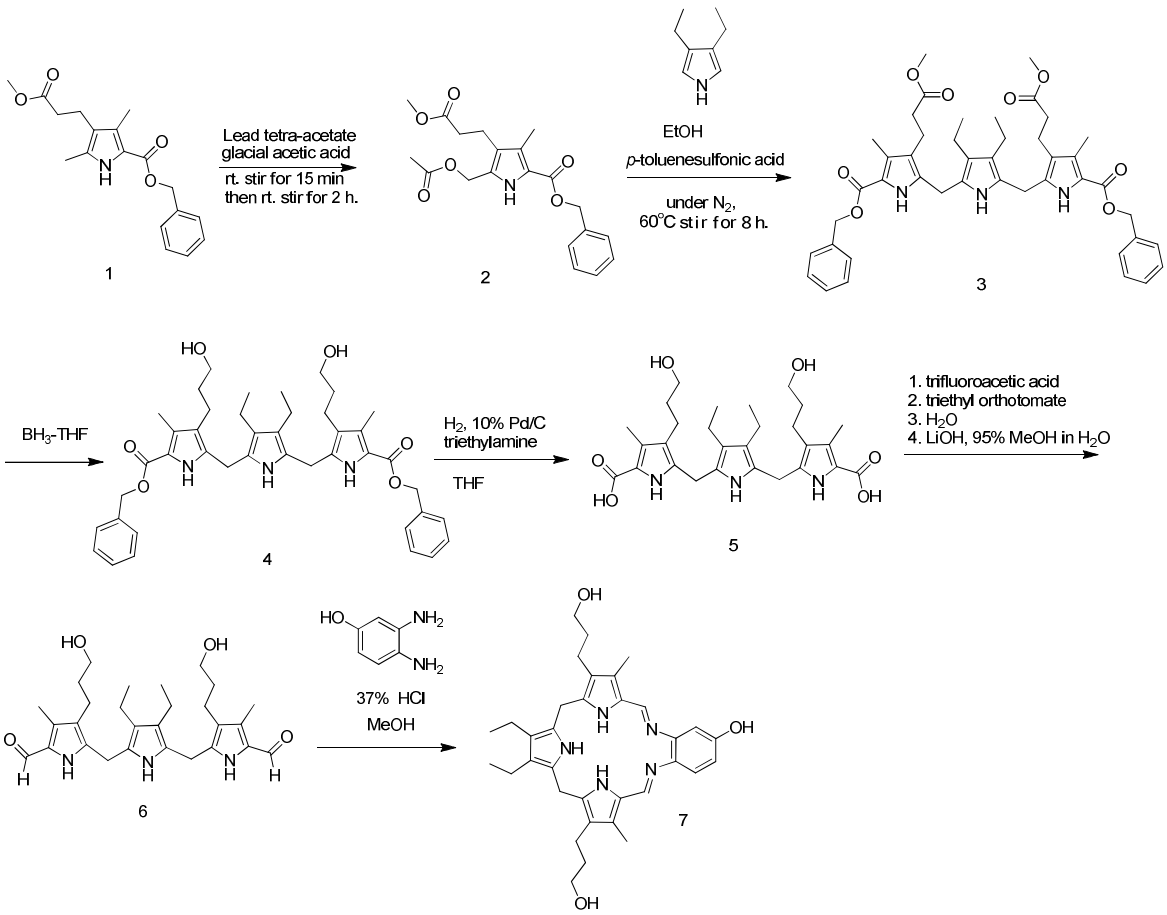

Scheme S-2. Synthesis procedures of texaphyrin.

Texaphyrin was synthesized according to references 1, 2 and3.

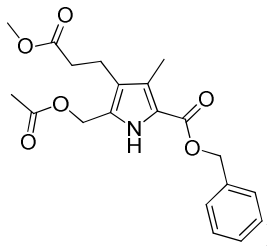

Synthesis of 2. Mol. Wt.:373.4. Lead tetra-acetate ($Pb(OAc)_4$) (2.45 g, 5.5 mmol) was added to a solution of benzyl 4-2'-methoxycarbonyl-ethyl-3,5-dimethylpyrole-2-carboxylate (compound **1**) (1.73 g, 5.5 mmol) in glacial acetic acid (25 mL) at room temperature in 15 min. After 2 h stirring, the solvent was removed under reduced pressure, and the residue

was poured into 50 mL water. The precipitated solid was separated, washed with water, and crystallised from aqueous acetone, it formed colourless needles in 69% yield.

Synthesis of 3: 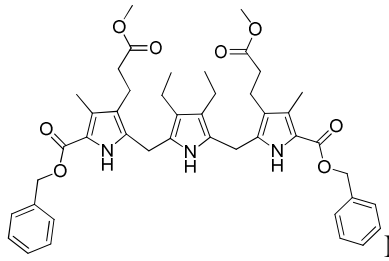 Mol. Wt.:749.89. 25 mL ethanolwas placed in a 50 mL round-bottom flask and purged with dry nitrogen for 10 min. Benzyl 5-A cetoxymethyl-4-2'-methoxycarbonylethyl-3-methylpyrrole-2-carboxylate (compound **2**, 0.747 g, 2 mmol) and 3,4-diethylpyrrole (0.129 g, 1 mmol) were added and the mixture heated at 60 ^{o}C until all of the pyrroles dissolved. p-toluenesulfonic acid (6.5 mg, 0.038 mmol) was added and the reaction temperature maintained at 60 ℃. The color of the mixture slowly changed from clear yellow to dark red with the product precipitating. After 10 h, the reaction was cooled to room temperature, and then the solvent volume was reduced to half by the rotary evaporator. The resulting slurry was placed in the freezer for several hours. The product was collected by filtration and washed with a small amount of cold ethanol to afford an off-white fine powder (Yield, 75%).

Synthesis of 4. 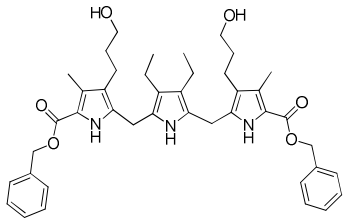 Mol. Wt.:693.87. 0.525 g of 2,5-Bis[(5-((benzyloxy)carbonyl)-4-methyl-3-(methoxycarbonyl)ethyl)pyrrol-2-yl)methyl]-3,4-diethyl-pyrrole (compound **3**, 0.7 mmol) was placed in a 100 mL three-necked round-bottom flask and vacuum dried for 30 min. The flask was equipped with an addition funnel, a thermometer, a

nitrogen inlet tube, and a magnetic stir bar. After the tripyrrane was partially dissolved into 10 ml of dry THF, 2.9 ml of borane (1 M BH_3 in THF) was added dropwise with stirring. The reaction became mildly exothermic and was cooled with a cool water bath. The dissolved tripyrrane formed a homogeneous orange solution which turned into a bright fluorescent orange color as the reaction completed. After being stirred for 1 h at room temperature, the reaction was quenched by adding methanol drop wise until the vigorous effervescence ceased. The solvent was removed under reduced pressure, and the resulting white solid was redissolved into CH_2Cl_2. The tripyrrane solution was washed three times with 0.5 M HCl (20 mL total), dried over anhydrous K_2CO_3, and filtered. The solvent was concentrated to a small volume under reduced pressure. After the addition of 50 mL hexanes, the flask of was transferred in to a freezer and the product would crystallize in several hours. The product was filtered and recrystallized in CH_2Cl_2/ethanol. The product was collected by filtration and vacuum dried to yield 0.412 g of an orange-tinted white solid (Yield, 85%).

Synthesis of 5. 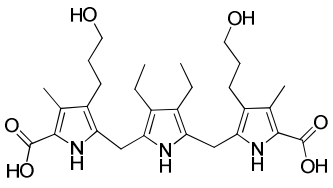 Mol. Wt.:513.67. 1.38 g of 2,5-Bis[(3-(3-hydroxypropyl)-5-((benzyloxy)-carbonyl)-4-methylpyrrol-2-yl)methyl]-3,4-diethylpyrrole (compound **4**, 2 mmol) was placed in a 250 mL round-bottom flask and dried in vacuo for ca. 30 min. The tripyrrane was dissolved in dry THF (60 ml) with triethylamine (10 drops) and 10% Pd on carbon (60 mg), and then stirred at room temperature under 1 atm of H_2. After 15 h, the suspension was filtered through Celite to remove the catalyst, and the resulting clear solution was concentrated under reduced pressure to yield a light pink solid. This material, obtained in near-quantitative yield, was taken to the next step without further purification.

Synthesis of 6. 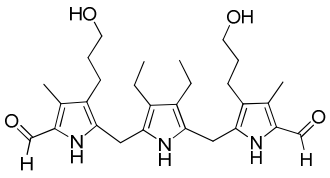 Mol. Wt.:481.63. 1.03g of 2,5-Bis[(3-(3-hydroxypropyl)-5-carboxyl-4-methylpyrrol-2-yl)methyl]-3,4-diethylpyrrole (compound **5**, 2 mmol) was placed in a 250 ml round-bottom flask and dried in vacuo for ca. 1 h. At room temperature, trifluoroacetic acid (3.1 mL, 40 mmol) was added drop wise via syringe under nitrogen. The tripyrrane dissolved with visible evolution of CO_2 formed a homogeneous yellow solution. The reaction was stirred at room temperature for ca. 15 min, then cooled to -20 ℃ using a dry ice/CCl_4 bath.

Freshly distilled triethyl orthoformate (3.1 mL, 20 mmol, dried over CaH_2) was added via a syringe to produce a dark orange/yellow solution. This mixture was further stirred for 10 min at -20℃. Then, the cold bath was removed and 10 mL of distilled water was added drop wise to the solution. The resulting brown suspension was stirred at room temperature for 15 min. The product was collected by filtration, washed several times with water and resuspended into a H_2O/EtOH/NH_4OH (5 mL/10 mL/5 mL, v/v/v) mixture. The yellow/brown suspension was stirred for 1 h, filtered, washed several times with water, and then rinsed with a small amount of cold ethanol.

At this point, TLC analysis showed a mixture of tripyrranes. Therefore, the crude dialdehyde tripyrrane and LiOH-H_2O (0.21 g, 5 mmol) were added to 40 ml of degassed 95% MeOH, and the suspension was refluxed under N_2 atmosphere. The reaction became homogeneous when heated. After ca. 1 h, it was slowly cooled to room temperature. The reaction mixture was concentrated under reduced pressure to 7.5 ml and the resulting slurry was placed in the freezer

for several hours. The product was filtered and then purified by forming slurry with 40 mL methanol and 5 mL water, and then heating close to boiling. The suspension was slowly cooled to room temperature, and the volume was reduced to 15 mL under reduced pressure, and placed in the freezer for several hours. The purified dialdehyde tripyrrane was filtered, rinsed with water and dried in vacuo for 24 h to yield 0.765 g (80%) of a light tan powder.

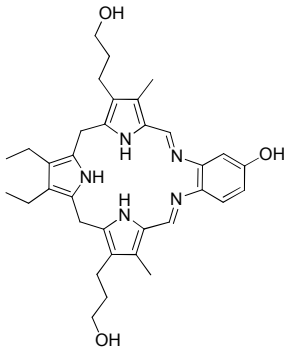

Synthesis of 7. Mol. Wt.:569.74. 0.96 g of 2,5-Bis[(5-formyl-3-(3-hydroxypropyl)-4-methylpyrrol-2-yl)methyl]-3,4-diethylpyrrole (compound **6**, 2 mmol) and 3,4-Diaminophenol (0.25 g, 2 mmol) were placed in a 2 L round-bottom flask with 1000 mL toluene and 200 mL methanol. The solvent was purged with nitrogen prior to use. Concentrated HCl (0.5 mL) was added and the reaction was heated to reflux under nitrogen. The color was changed from a clear suspension to a dark red homogeneous solution as the reaction proceeded. After 5 h, the reaction was cooled to room temperature and the solvent was removed under reduced pressure until the product precipitated out of solution. The remained solvent was decanted off and the macrocycle dried in vacuo. The dark red product was recrystallized from methanol/diethylether and yielded 1.4-1.5 g (90-100%).

Figure S-2 shows the ^{1}H NMR (Methanol-d_4, 500 MHz) of texaphyrin: δ 8.26 (s, 1H), 8.21 (s, 1H), 7.60 (d, J = 10 Hz, 1H), 7.19 (d, J = 5 Hz, 1H), 6.92 (dd, J = 10, 5 Hz, 1H), 4.12 (d, 4H),

3.61 (t, J = 6.1 Hz, 4H), 2.62-2.68 (m, 4H), 2.45-2.52 (m, 4H), 2.35 (s, 3H), 2.33 (s, 3H), 1.81-1.72 (m, 4H), 1.10-1.18 (m, 6H).

Figure S-3 shows the high resolution MS (ESI) of texaphyrin: m/z calcd for $C_{34}H_{44}N_5O_3$ 570.3444 $[M+H]^+$, found 570.3751 $[M+H]^+$.

Synthesis of Gd-texaphyrin (Gd-TP). Texaphyrin (35 mg, 0.061 mmol) was dissolved in 30 mL methanol, and then $GdCl_3 \cdot 3H_2O$（58 mg, 0.183 mmol）and trimethylamine (ca. 0.2 mL) was added, the mixture was heated at reflux for 7 h. After completion, the reaction was cooled to room temperature, the solvent was removed in vacuo, and the results light green solid was recrystallized from MeOH/CH_2Cl_2/Et_2O, 20 mg of a light green powder was obtained, yielded 41%. The ^1H NMR spectrum of the compound was broadened and useless for structural identification. Therefore the compound was characterized by UV-Vis spectroscopy and high resolution mass spectroscopy. UV/vis (MeOH, 25 °C) :

Figure S-4 shows the high resolution MS (ESI) of Gd-TP: m/z calculated for $C_{34}H_{38}Cl_2GdN_5O_3$ $[M-Cl]^+$ 757.1904, found 757.1900.

Synthesis of Lu-texaphyrin (Lu-TP). Texaphyrin (20 mg, 0.035 mmol) was dissolved in 30 mL methanol, and then $Lu(NO_3)_3 \cdot H_2O$ (39.8 mg, 0.105 mmol) and trimethylamine (ca. 0.02 mL) was added, the mixture was heated at reflux for 24 h. After completion, the reaction was cooled to room temperature, the solvent was removed in vacuo, and the resulting light tan solid was recrystallized from MeOH/CH_2Cl_2/Et_2O, 10 mg of a light tan powder was obtained, yield 33%.

Figure S-5 shows the high resolution MS (ESI) of Lu-TP: m/z calculated for $C_{34}H_{38}LuN_7O_9$ $[M+CH_3CN+H+1]^+$ 906.2477, found 906.2542.

Loading of Lu-TP and/or Gd-TP on GQD-RGD. GQD-RGD, Lu-texaphyrin and/or Gd-texaphyrin were mixed in a distilled water/DMSO solution by sonication, the mixture was further stirred overnight in dark at room temperature. The obtained mixture was dialyzed against DI water to remove free DMSO. Unbounded Lu-texaphyrin and/or Gd-texaphyrin were dislodged by centrifugation at 5000 rpm/min for 3 min. Concentration of the formed Lu-TP&Gd-TP/GQD-RGD complex solution was carried out by ultrafiltration in an ultra-centrifugal filter (Millipore, 3 K) at 5000 rpm for 20 min. The resulting Lu-TP&Gd-TP/GQD-RGD aqueous solution was preserved in darkness at 4 °C.

The UV-vis spectrum of the obtained aqueous solution showed typical peaks of Lu-TP, Gd-TP and GQD-RGD (Figure S-6), suggesting the successful loading of water insoluble drugs on GQD-RGD through π–π stacking and the hydrophobic effect. The designed probe could be well-dispersed in water at weight ratios less than 36%. It is likely that the increased hydrophobicity may cause aggregation at higher metal-texaphyrin content. The dispersion status was also investigated; results showed that 6 mg of the nanoconstruct (30% by weight) could stably disperse in 1 mL water, PBS, DMEM cell medium or 10% serum over a month of storage at 4 °C (Figure S-7).

The interaction between the drugs and vehicles was studied by recording their typical fluorescence emission. Figure S-8 indicates that GQD and GQD-RGD both exhibited a maximum emission of ~582 nm upon excitation at 490 nm. The emission peak of GQD-RGD shifted towards the near-infrared region as the excitation wavelength varied from 430 nm to 560 nm, while the two drugs sustained their characteristic peak as the excitation wavelength increased (Figure S-9).

The content of Gd-TP and Lu-TP on the Lu-TP&Gd-TP/GQD-RGD nanoconstruct was quantified by inductively coupled plasma-mass spectrometry (ICP-MS). In a typical ICP-MS procedure, 100 μL of the formed Lu-TP&Gd-TP/GQD-RGD aqueous solution was added to 9.9 mL of 4% HNO_3 aqueous solution. The mixture was sonicated for 10 min, and then heated to 100 °C for 2 h. After cooling to room temperature, the obtained mixture was diluted to 10 mL, and then filtered through a 0.22 μm microporous filter. The standard solutions with gadolinium or lutetium concentration of 1, 5, 10, 20, 50, 100, 200 ppm in 3% nitric acid were prepared, and a calibration curve was made by plotting the corresponding chromatographic peaks vs. gadolinium or lutetium concentrations. The Gd-TP and Lu-TP content was obtained by applying the detected gadolinium or lutetium peaks against the calibration curve.

Detection of $^1O_2$ generation. Photosensitizers can selectively damage irradiated cancer cells, while leaving healthy cells unaffected, by generating ROS or reacting with some oxidatively biological substrates under laser irradiation. We investigated singlet oxygen ($^1O_2$) generation by Lu-TP & Gd-TP/GQD-RGD under irradiation at 765 nm. According to Kraljic et al., the presence of $^1O_2$ in aqueous solutions could be sensitively and selectively tested by combined use of acceptor imidazole and scavengerp-nitrosodimethylaniline (RNO).[4] In this experiment, GQD-RGD, Gd-TP/GQD-RGD (0.15 μM Gd-TP), Lu-TP/GQD-RGD (0.15 μM Lu-TP) and Lu-TP&Gd-TP/GQD-RGD (nLu: nGd = 2:1, 0.15 μM of texaphyrin) were added to a PBS 7.4buffer solution which contained 25 μM imidazole and 25 μM RNO, respectively. The mixed solutions were then irradiated by 765 nm laser light at a power density of 50 mW/cm^2 for different periods of time. The generation of $^1O_2$ was estimated by detecting the decrease of RNO absorption at 440 nm.

As the irradiation time increased, the generation of $^1O_2$ was slightly increased in the absence of Gd-TP/GQD-RGD (Figure S-10). Lu-TP/GQD-RGD and Lu-TP & Gd-TP/GQD-RGD exhibited a much more pronounced increase. In view of the above results, we conclude that Lu-TP is the primary cause of singlet oxygen generation by Lu-TP & Gd-TP/GQD-RGD.

***In vitro* photodynamic treatment (PDT)**

Cellular uptake of Lu-TP&Gd-TP/GQD-RGD and PDT. A549 cells were maintained in DMEM medium, supplemented with 10% inactivated fetal bovine serum and 1% penicillin/streptomycin 10000 U/ml, and was grown in an incubator at 37°C, supplied with 5% CO_2.

For the cellular uptake of the designed nanoprobe, A549 cells at a density of 2×10^6 /mL were seeded in a 6-well chamber slide with one piece of cover glass at the bottom of each chamber. After 12 h plating, solutions of GQD-RGD, Gd-TP/GQD-RGD, Lu-TP/GQD-RGD, and Lu-TP& Gd-TP/GQD-RGD were added respectively. After 4 h incubation, the cells were irradiated using the 765 nm laser at a power density of 50 mW/cm^2 for 4 min (laser dose 12 J/cm^2). Then, the cells were washed with PBS 7.4 for three times to remove extra solution. The cells were further incubated in cell medium DMEM at 37°C for 24 h. To achieve fixation, cells were immersed in 4% paraformaldehyde in PBS for 10 min, at room temperature. Following fixation, the slides were washed three times with distilled water and visualized under a laser scanning confocal microscope Nikon A1.

Gd-TP/GQD-RGD localized in the cytoplasm and perinuclear region of A549 cells (Figure S-11, 12). Both the light treated (Figure S-11) and untreated cells (Figure S12) attached well and were spindle shaped, illustrating that Gd-TP/GQD-RGD treated cells did not show obvious

response to light treatment (Figure S-11). After irradiation, the Lu-TP/GQD-RGD treated cells located within the laser-irradiated area were found to be loosely attached, rounded and randomly oriented (Figure S-11, yellow cycles). Meanwhile, fluorescence from nanoconstructs was observed in the nucleus of some irradiated cells, indicating that their nuclear membrane was likely damaged by PDT. Only a small amount of Lu-TP & Gd-TP/GQD-RGD treated A549 cells were observed in laser-irradiated area (Figure S-11) because these adherent cells were killed and separated from the substrates by redox perturbations together with the PDT process. Meanwhile, cells treated with the three different probes remained and attached well in the region outside the laser footprint. The above results confirm the PDT response from Lu-TP is accelerated by the addition of Gd-TP.

Live/dead cell viability assay. To better demonstrate how Gd-TP enhances the PDT induced by Lu-TP, a live/dead cell assay was introduced to understand the mechanisms of cytotoxicity, apoptosis and/or necrosis. To directly determine the viability of A549 cells after PDT, the morphology of nuclear chromatin was assessed bystaining with two fluorescent dyes,membrane permeable dye Hoechst 33342 and membrane impermeable dye sytox Green. Cultured and irradiated cells were washed with PBS 7.4, then stained with Hoechst 33342 (10 μg/ml) and sytox Green (10 μg/ml) for 30 min at 37 °C. Cells were washed again with PBS 7.4 and fixed with 4% paraformaldehyde.

After irradiation, A549 cells treated with GQD-RGD were evidently viable (Hoechst 33342+/Sytox green+). In contrast, apoptosis (Hoechst 33342++/Sytox green+) was observed in cancer cells treated with Gd-TP/GQD-RGD, indicating the toxicity of the biological redox drug to cancer cells. Cells treated with Lu-TP/GQD-RGD were mostly apoptotic, and in some cases even necrotic (Hoechst 33342+/sytox green++), indicating the activation of the photosensitizer

by light. Moreover, most of the irradiated cells with Lu-TP&Gd-TP/GQD-RGD treatment were necrotic. These results further corroborate the hypothesis that the addition of redox active drug Gd-TP promotes apoptosis and/or necrosis in PDT. Moreover, cells that were not irradiated remained viable for the most part, suggesting Lu-TP/GQD-RGD and Lu-TP & Gd-TP/GQD-RGD exhibited negligible dark toxicity to A549 cells.

Annexin V-FITC/PI apoptosis detection. A549 cells at a density of 5×10^6 /mL were seeded in a 6-well chamber. After 12 h plating, solutions of GQD-RGD, Gd-TP/GQD-RGD, Lu-TP/GQD-RGD, and Lu-TP& Gd-TP/GQD-RGD were added respectively. After 4 h incubation, the cells were irradiated using the 765 nm laser at a power density of 50 mW/cm^2 for 4 min. Then, the cells were washed with PBS 7.4 three times to remove extra solution. The cells were further incubated in cell medium DMEM at 37°C for 10 h. Then, cells were digested by trypsin (without EDTA), spined down at 1,000 to 2,000 rpm for five minutes, and re-dispered in 0.5 mL PBS.

Cell concentration was generated to $2\sim3\times10^6$ cells/mL by the Cellometer Sample Adjustment Calculator. 40 μL of the cells was transferred into a new tube, followed by adding 5 μL of Annexin V-FITC and 5 μL of PI solution. The sample was mixed by gently pipetting up and down 10 times, and then incubated for 15 min at room temperature in the dark. The apoptosis and necrosis of the prepared cells were mearsured at the Cellometer K2 Image Cytometer by CBA_Annexin V + PI assay.

Selective delivery and damage. A549 and MCF7 cells at a density of 1×10^6 /mL were seeded respectively in a 6-well chamber slide with one piece of cover glass at the bottom of each chamber, and were grown in DMEM containing 10% fetal bovine serumand 1%

penicillin/streptomycinat 37ºC overnight. To help visually distinguish the two different types of cells, A549 and MCF7 cells were labeled with DiSC3 (Ex/Em 660/675 nm) andDiO (Ex/Em 484/501 nm), respectively. The labeled cells were incubated with Lu-TP&Gd-TP/GQD-RGD for 30 min respectively, and then irradiated with a 765 nm laser. All the PDT experimental conditions were the same as described in 2.1.

For the cell mixture experiment, A549 cells and MCF7 cells were labeled with DiSC3 and DiO as described. Then the two types of cells were separated from the substrates respectively by trysinization. The digested cells were centrifuged and redispersed in DMEM with 10% inactivated fetal bovine serum and 1% penicillin/streptomycin 10000 U/ml. The concentration of cells was confirmed by a cellometer. Then, a 1:1 cell mixture of A549 cells and MCF7 cells was seeded in a 6-well chamber slide with one piece of cover glass, and seeded overnight. The mixed cells also incubated with Lu-TP&Gd-TP/GQD-RGD for 30 min, and irradiated with a 765 nm laser.

***In vivo* treatment**

Tumor implantation. Adult female nude mice (average 20 g) were obtained from Hunan SJA Laboratory Animal Co., Ltd (Changsha, China). All experiments conformed to animal care protocols and were approved by Animal Care and Use Committees at the Wuhan Institute of Physics and Mathematics, the Chinese Academy of Sciences. To induce a tumor, ~2×10^6 A549 cells were suspended into 200 μL PBS and injected into the front back of lightly anesthetized mice (1% isoflurane/oxygen mixture).

***In vivo* MRI.** Imaging was performed on a 7 T, small-animal horizontal bore system (Bruker BioSpec; Bruker, Billerica, MA). 12-cm-diameter Helmholtz coil arrangement served for rf

excitation, whereas signal detection was achieved with a 23-mm diameter surface coil. The coils were decoupled from each other. Gradients used in the magnet were 12 cm diameter at 25 G/cm. Imaging was performed using a custom-built 50 mm diameter send-receive birdcage volume coil. Following induction of a mouse to anesthesia using 4% isoflurane/oxygen, mice were fixed to an acrylic patient bed in the prone position and maintained on a 1% isoflurane/oxygen mixture. Body temperature was monitored with a platinum rectal probe connected to a small-animal monitoring system (SA Incorporated) and maintained using a stream of heated air. T1-weighted images were acquired in the axial plane using a multi-slice spin-echo sequence with the following parameters: TR/TE = 400/11 milliseconds, matrix =128 ×128, FOV (field of view) = 30 ×30 mm, slice thickness = 1 mm, NEX (number of excitations) = 4. Scans were completed before and after intravenous injection of Lu-TP& Gd-TP/GQD-RGD aqueous solution via tail vein.

***In vivo* fluorescence imaging.** To further investigate the in vivo targeting ability and fluorescence imaging property, we administered the fabricated probe to nude mice which was transplanted with A549 cancer cells. According to the emission spectrum, the probe Lu-TP&Gd-TP/GQD-RGD has two inherent peaks, one from the GQD vehicle at 582 nm, the other from the carried drugs at 782 nm. It is well known that in vivo autofluorescence from hemoglobin is rather strong around 600 nm. In order to decrease background noise, we chose the near infrared fluorescence around 780 nm to track the in vivo targeting ability of the designed probe.

Lu-TP&Gd-TP/GQD-RGD aqueous solution was intravenously injected via tail vein after the nude mice was anaesthetized by peritoneal injection of pelltobarbitalum natricum at a concentration of 50 $mg \cdot kg^{-1}$. The mouse was then transferred into the Bruker imaging system, a

laser of 710 nm was applied to excite the probe. Fluorescence imaging photographs were acquired every ten minutes to monitor the location of the injected probes.

In vivo **photodynamic therapy.** To evaluate the in vivo PDT efficiency, probes were intravenously injected into nude mice with ~ 5 mm tumor via tail vein. At 1.5 h post-injection, the mice were anaesthetized by peritoneal injection of pelltobarbitalum natricum and the tumor area was irradiated with a 765 nm laser for 20 min. The laser power was measured to be 300 mW with a spot size of 1 cm diameter.

A549 tumor-bearing mice were divided into 6 groups of five animals per group to quantify the growth rate of tumors after the following treatments: i) physiological saline administrated and irradiated; ii) Gd-TP/GQD-RGD aqueous solution administrated and irradiated; iii) Lu-TP/GQD-RGD aqueous solution administrated and irradiated; iv) Lu-TP&Gd-TP/GQD-RGD aqueous solution administrated, no irradiation; v) Lu-TP&Gd-TP/GQD-RGD aqueous solution administrated and irradiated. The mice were treated every 7th day, and all the groups were treated for three periods.

Tumor size was measured by MRI before treatment. The volume of tumor (V) was calculated by the following equation: $\boldsymbol{V=A\times B\times C}$, where A and B are the length and width diameter (mm) of the tumor respectively, which could be accurately calculated from the maximum transverse section of the tumor across the MRI scans. C is the height of tumor; the latter was estimated from the number of MRI slices containing the tumor.

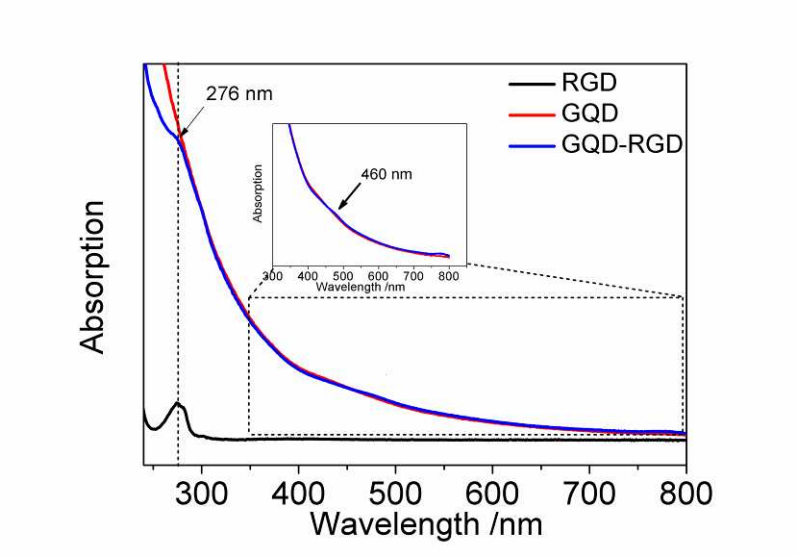

Figure S-1. UV-vis spectra of RGD, GQD and GQD-RGD.

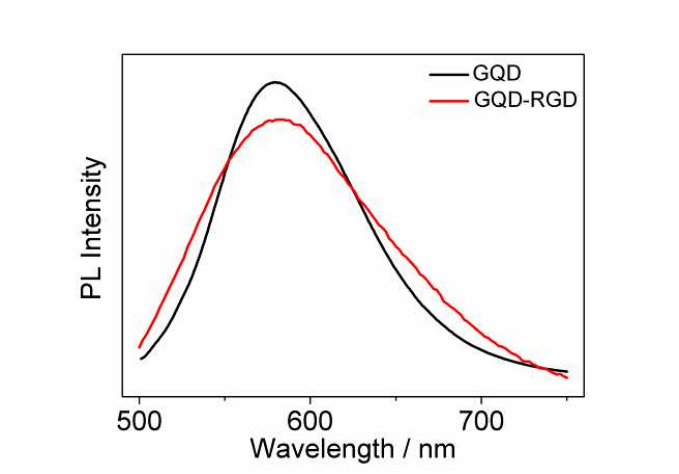

Figure S-2. Photoluminescence spectra of GQD and GQD-RGD aqueous solution under an exciting wavelength of 490 nm.

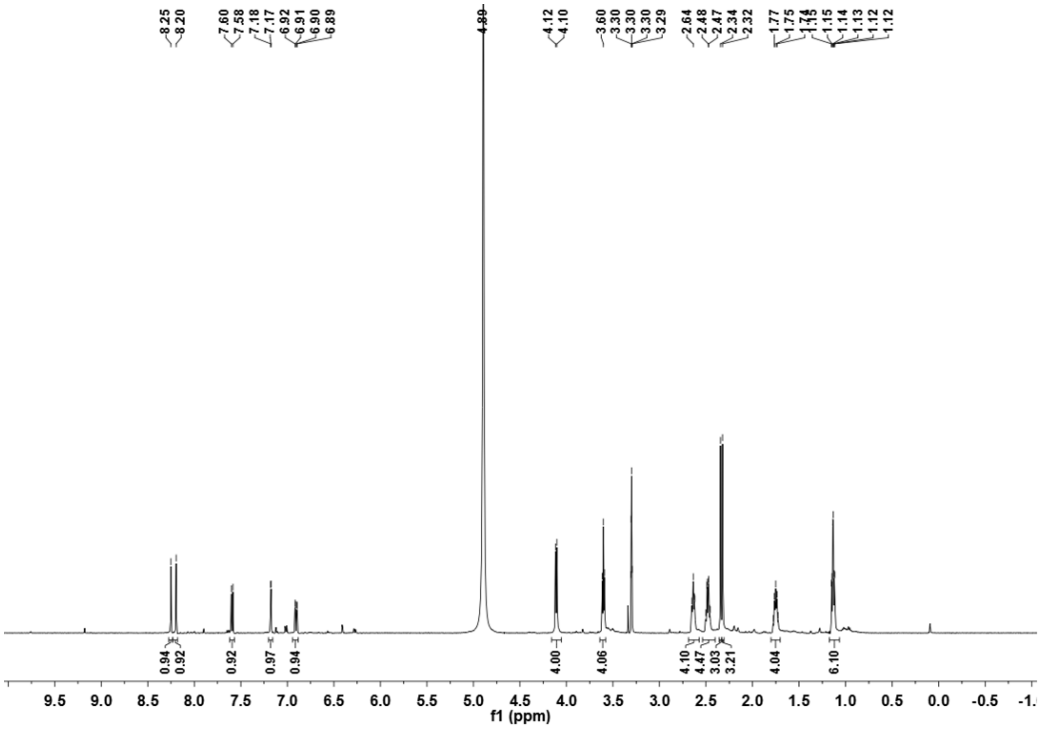

Figure S-3. ^{1}H NMR of texaphyrin.

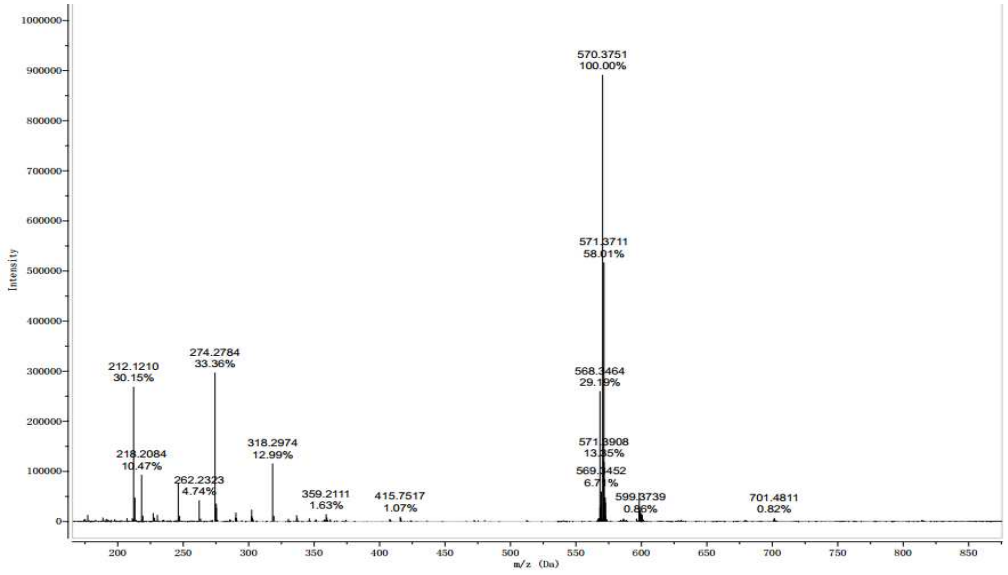

Figure S-4. High-resolution mass spectra of texaphyrin.

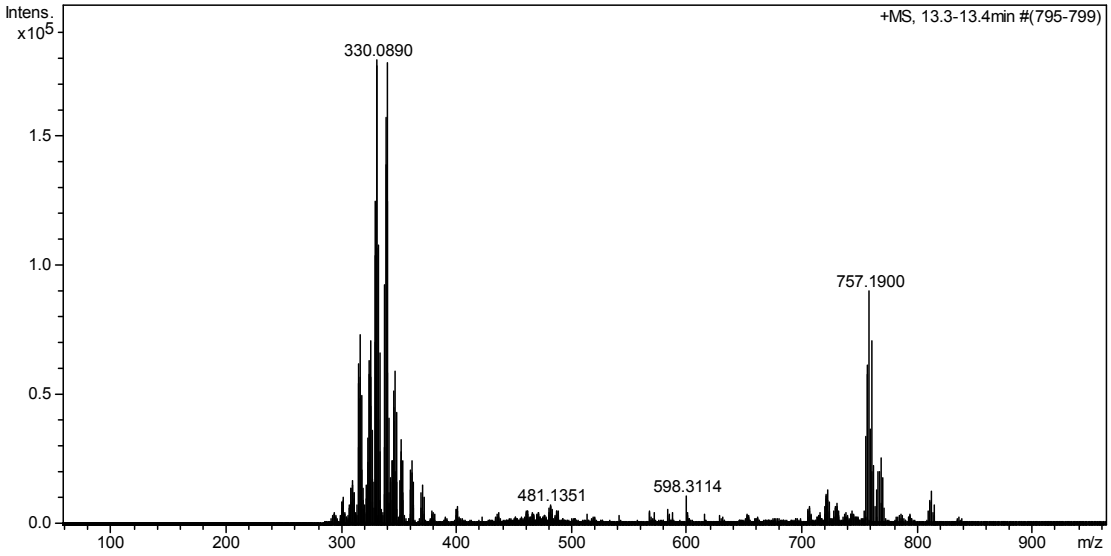

Figure S-5. High-resolution mass spectra of Gd-texaphyrin.

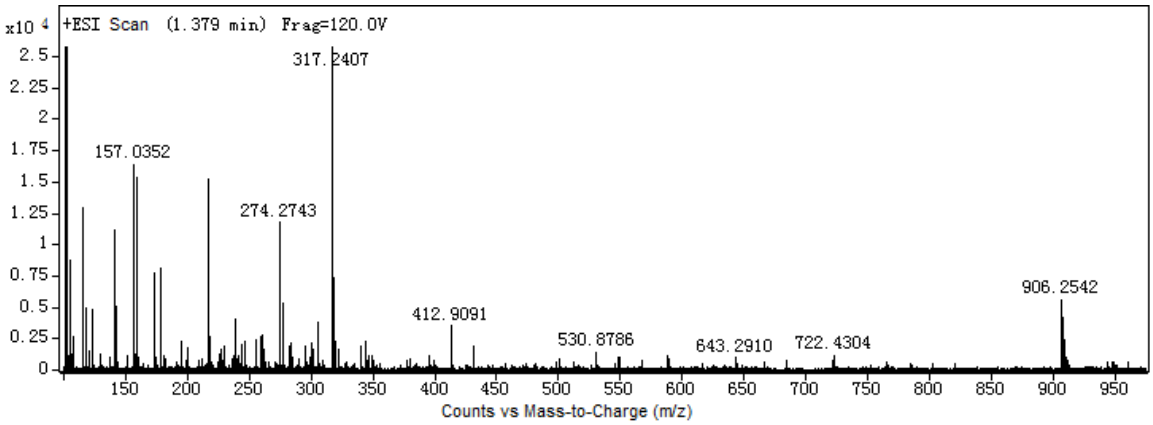

Figure S-6. High-resolution Mass mass spectra of Lu-texaphyrin.

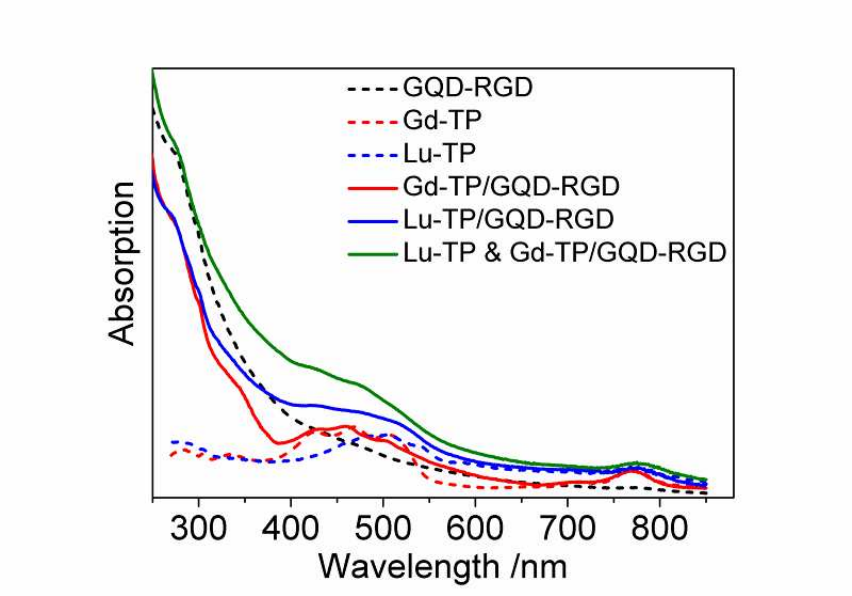

Figure S-7. UV−vis spectra of GQD-RGD (dashed black line), Gd-TP (dashed red line), Lu-TP (dashed blue line), Gd-TP/GQD-RGD (solid red line), Lu-TP/GQD-RGD (solid blue line) and Lu -TP&Gd-TP/GQD-RGD (solid green line).

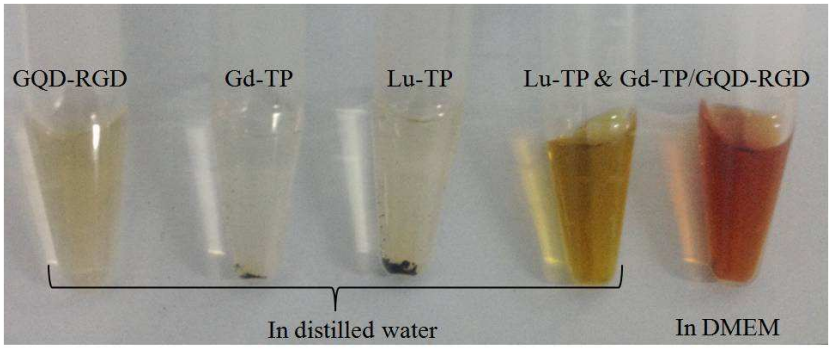

Figure S-8. Photographs of GQD-RGD, Gd-TP, Lu-TP, Lu-TP&Gd-TP/GQD-RGD in distilled water and Lu-TP&Gd-TP/GQD-RGD in cell-culture medium DMEM.

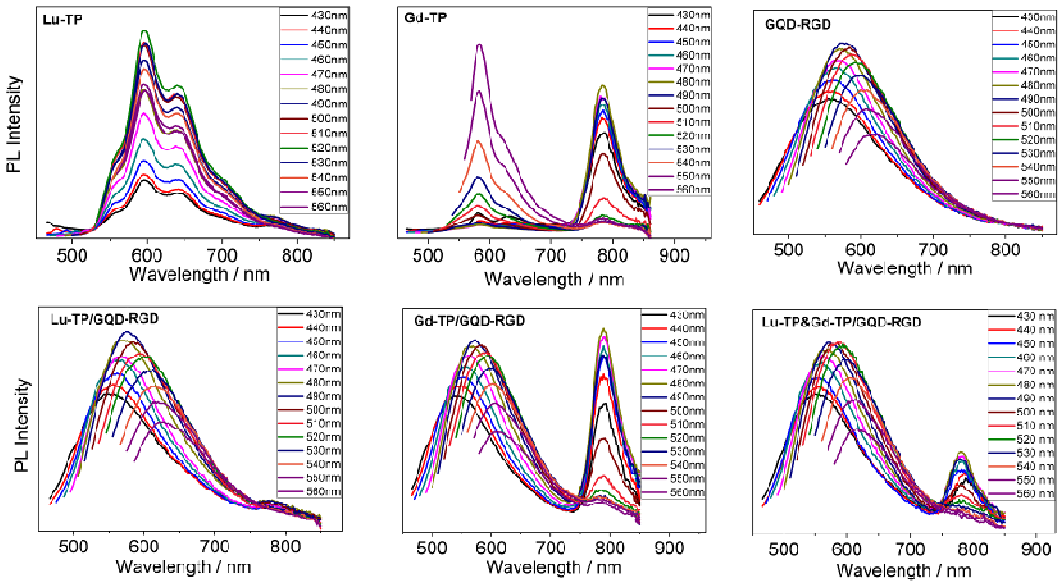

Figure S-9. Photoluminescence spectra of GQD-RGD, Gd-TP, Lu-TP, Gd-TP/GQD-RGD, Lu-TP/GQD-RGD and Lu -TP&Gd-TP/GQD-RGD.

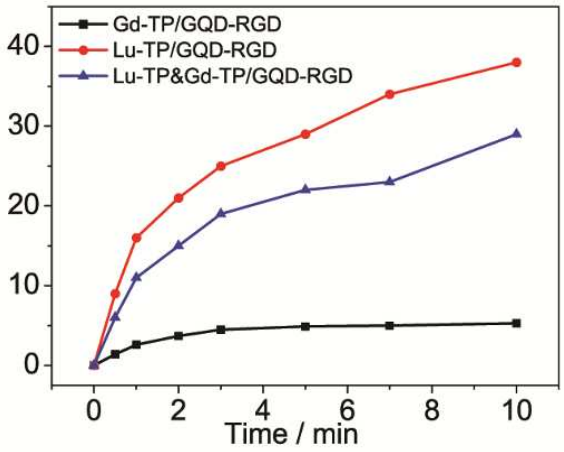

Figure S-10. Time-course generation of singlet oxygen by Gd-TP/GQD-RGD (red line), Lu-TP/GQD-RGD (blue line) and Lu-TP&Gd-TP/GQD-RGD (black line) at 2 μM of texaphyrin equivalent under 765 nm laser irradiation (50 mW/cm^2).

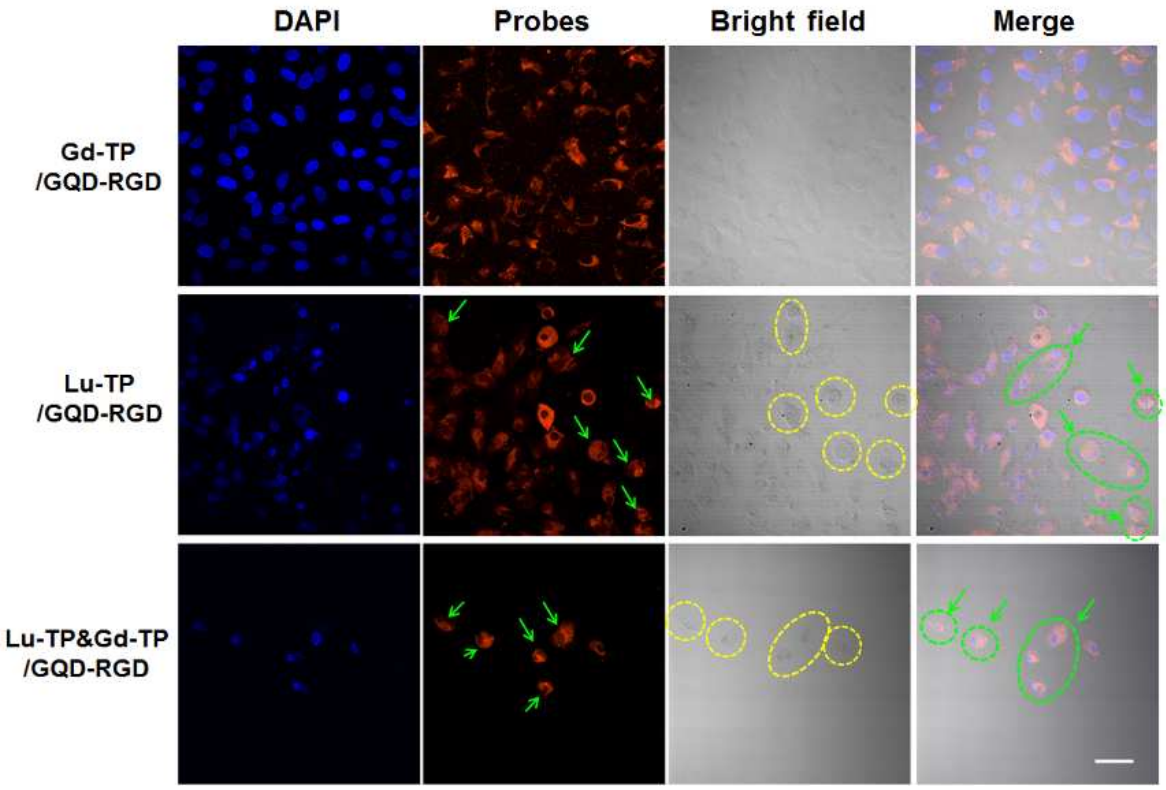

Figure S-11. CLSM images of Gd-TP/GQD, Lu-TP/GQD and Lu-TP&Gd-TP/GQD-RGD treated A549 cells in irradiated region. Laser power intensity: 50 mW/cm^2, laser time: 4min (12 J/cm^2). Scale bar, 50 μm.

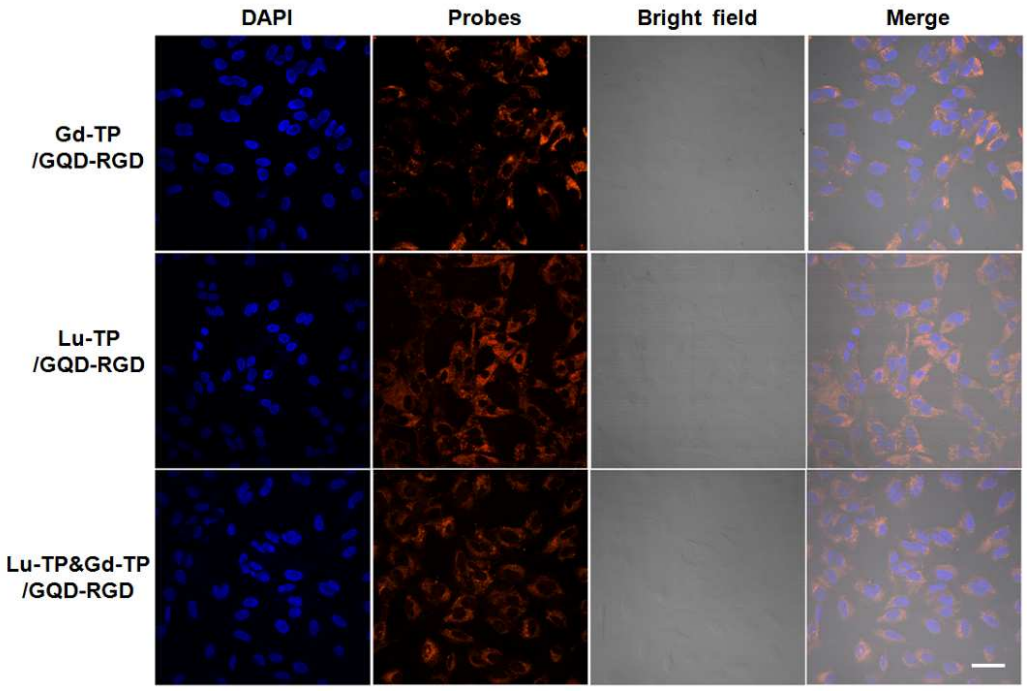

Figure S-12. CLSM images of Gd-TP/GQD-RGD, Lu-TP/GQD-RGD and Lu-TP&Gd-TP/GQD-RGD treated A549 cells in unirradiated region. Scale bar, 50 μm.

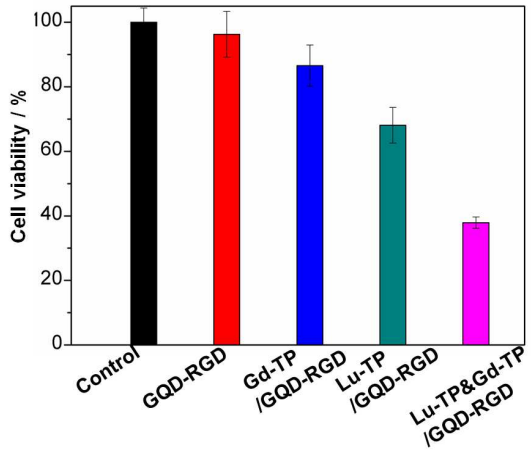

Figure S-13. Cell viability of GQD-RGD, Gd-TP/GQD-RGD, Lu-TP/GQD-RGD and Lu-TP&Gd-TP/GQD-RGD treated A549 cells.

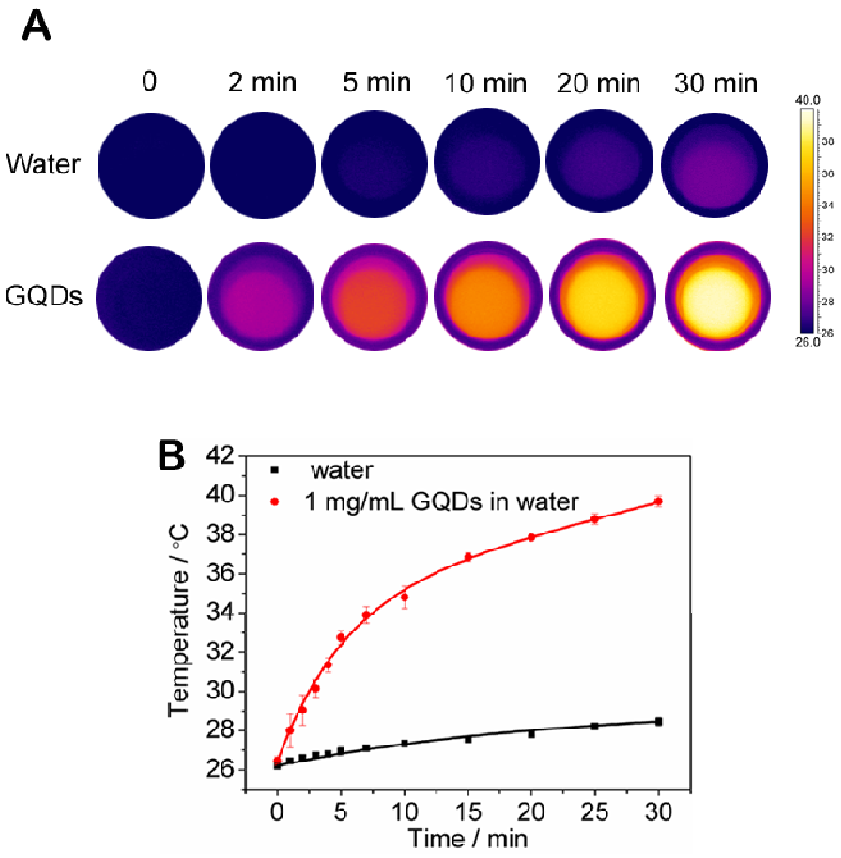

Figure S-14. (A) Thermal images and (B) temperature change of distilled water and GQD aqueous solution after irradiated under a 765 nm laser at a power of 300 mW/cm^2.

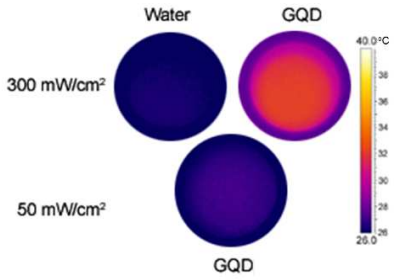

Figure S-15. Thermal images of water and GQD aqueous solution after 4 min irradiation with a 765 nm laser at power of 300 mW/cm^2 or 50 mW/cm^2.

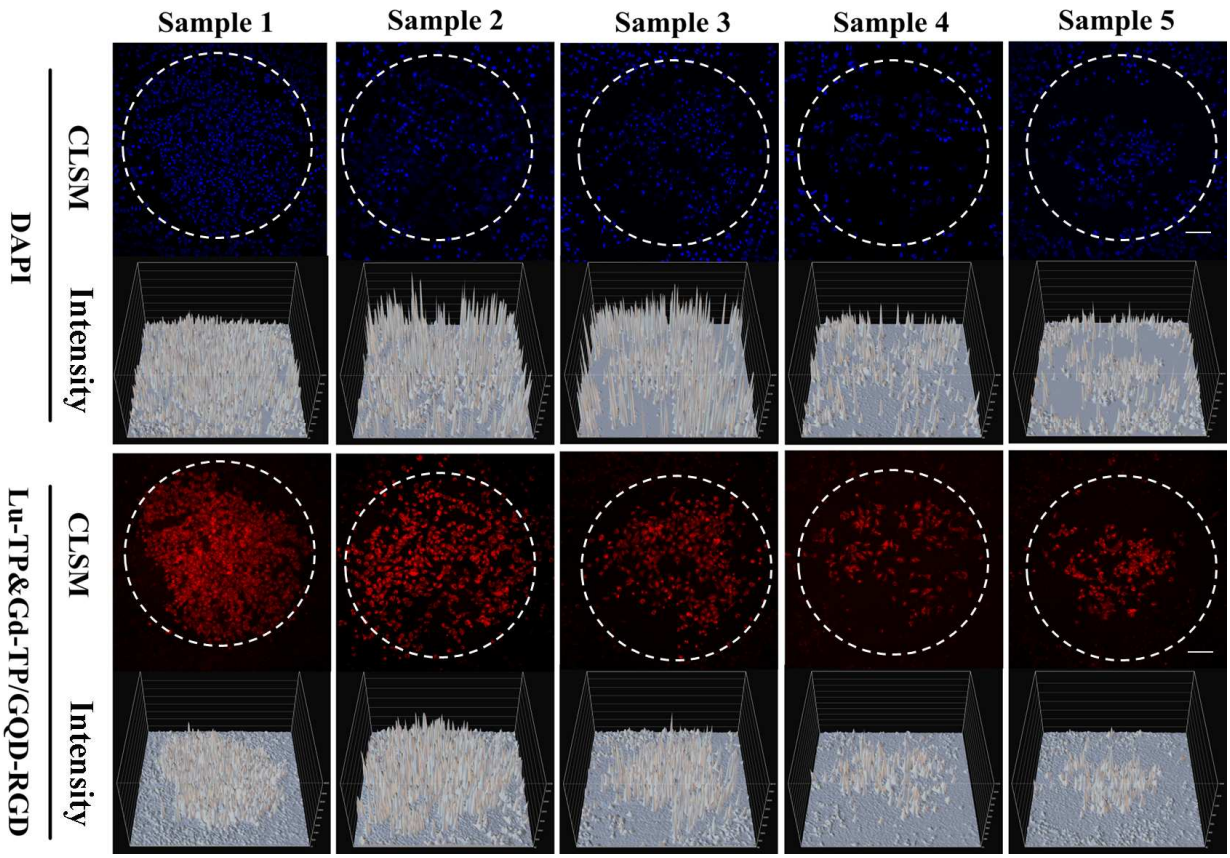

Figure S-16. Confocal laser scanning microscope (CLSM) and fluorescence intensity of Lu-TP&Gd-TP/GQD-RGD incubated A549 cells. Sample 1, sample 2, sample 3, sample 4, sample 5 were further cultured for 2, 4, 6, 8, 10 h after laser irradiation. A mask was employed to confine the laser beam to a circular region with a diameter of 1 mm (as indicated by the white dashed circles). Scale bar, 100μm.

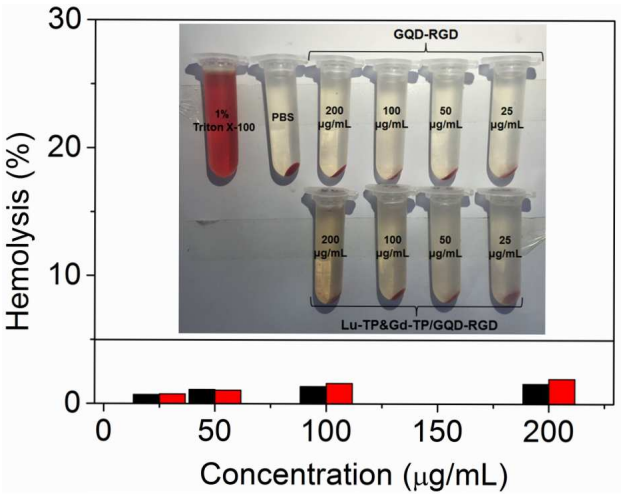

Figure S-17. Hemolysis of GQD-RGD and Lu-TP&Gd-TP/GQD-RGD with PBS as a negative control and 1% of Triton X-100 water as a positive control. Inset shows photograph of GQD-RGD and Lu-TP&Gd-TP/GQD-RGD with different concentrations, positive and negative control after centrifugation.

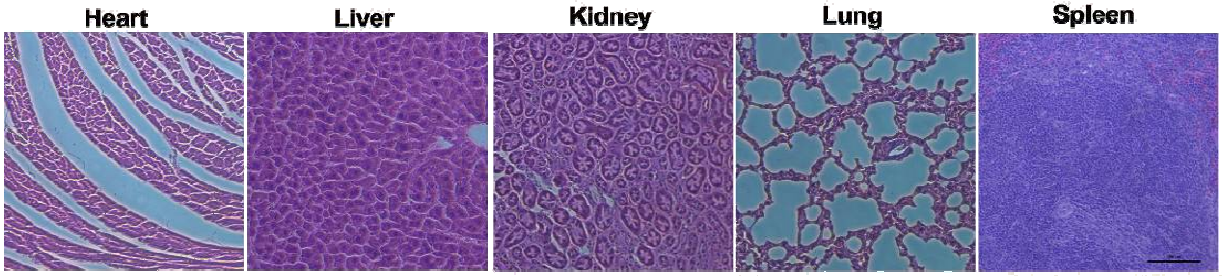

Figure S-18. Haematoxylin and eosin (H&E) stains of heart, liver, kidney, lung and spleen from Lu-TP&Gd-TP/GQD-RGD and laser treated group. Scale bar, 100 μm.

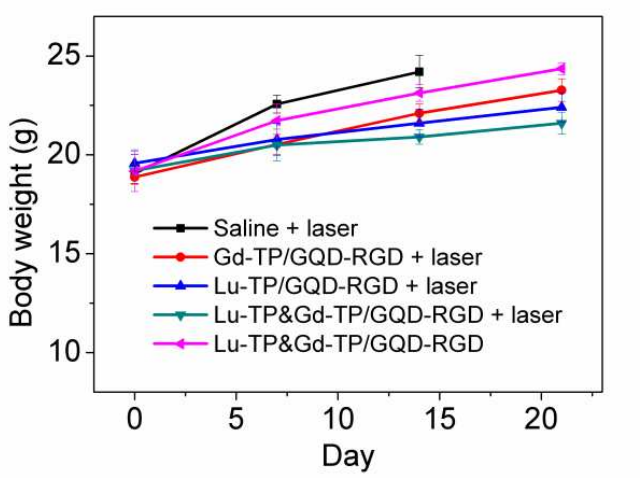

Figure S-19. Mean body weights of mice in different groups after treatment.

REFERENCES:

(1) Johnson, A. W.; Kay, I. T.; Markham, E.; Price, R.; Shaw, K. B. Colouring Matters Derived from Pyrroles. Part II. Improved Syntheses of some Dipyrromethenes and Porphyrins. *J. Chem. Soc.* **1959**, 11, 3416-3424.

(2) Sessler, J. L.; Mody, T. D.; Hemmi, G. W.; Lynch, V. Synthesis and Structural Characterization of Lanthanide(III) Texaphyrins. *Inorg. Chem.* **1993**, 32, 3175-3187.

(3) Sessler, J. L.; Mody, T. D.; Lynch, V. Synthesis and Crystal Structure of a Novel Tripyrrane-containing Porphyrinogen-like Macrocycle. *J. Org. Chem.* **1987**, 52, 4394-4397.

(4) Kraljić, I.; Mohsni, S. E. A New Method for the Detection of Singlet Oxygen in Aqueous Solutions. *Photochem Photobiol.* **1978**, 28, 577-581.